IEEE Access
Multidisciplinary | Rapid Review | Open Access Journal

Received October 10, 2021, accepted October 18, 2021, date of publication October 21, 2021, date of current version October 27, 2021.

Digital Object Identifier 10.1109/ACCESS.2021.3121880

Detection of Open Conductor Fault Using Multiple Measurement Factors of Feeder RTUs in Power Distribution Networks With DGs

JI-SONG HONG[1], (Graduate Student Member, IEEE), SEUNG-YOON HYUN[2], YOUNG-WOO LEE[1], (Member, IEEE), JOON-HO CHOI[1], (Member, IEEE), SEON-JU AHN[1], (Member, IEEE), AND SANG-YUN YUN[1], (Member, IEEE)

[1]Department of Electrical Engineering, Chonnam National University, Gwangju 61186, South Korea
[2]KEPCO Research Institute, Korea Electric Power Corporation, Yuseong-Gu, Daejeon 34056, South Korea

Corresponding author: Sang-Yun Yun (drk9034@chonnam.ac.kr)

This work was supported in part by Korea Electric Power Corporation through the KEPCO Research Institute under Grant R20DA25, in part by the Korea Institute of Energy Technology Evaluation and Planning (KETEP), and in part by the Ministry of Trade, Industry and Energy (MOTIE) of the Republic of Korea under Grant 2019381010001B.

ABSTRACT Open conductor faults are causing socioeconomic problems worldwide owing to fires caused by arc generation and increased risk of human electric shock. Also, the recent increase in the interconnection of distributed generators (DGs) has further aggravated the difficulty in detecting open conductor faults. In this study, we proposed a detection method for open conductor faults in power distribution networks using multivariate measurement factors of feeder remote terminal units (RTUs). The proposed method has the following advantages over the existing methods. First, the applicability in actual networks has been secured by utilizing the measurement values detectable in a general RTU. We analyzed the characteristics of open conductor faults according to the fault type, transformer connection, DG, etc., which we devised detection procedures for RTUs at the source-side and load-side of the open conductor point and developed an algorithm for open conductor detection. Using the proposed detection method, each RTU derived three results of open conductor alarm, warning, and no detection. Second, the detection problem caused by the DG in the existing open conductor method was rectified. Also, the limitations of classification between open conductor fault and other events were improved. Simulations using Matlab Simulink for a standardized power distribution network proved that the proposed method has a higher open conductor detection rate and distinguishing capability compared to the existing methods. Lastly, we demonstrated the applicability of the proposed method to a real system by deriving the optimal detection criteria using a sensitivity analysis.

INDEX TERMS Open conductor fault, high impedance fault, feeder remote terminal unit, rule-based detection method, power distribution network, sensitivity analysis.

I. INTRODUCTION

An open conductor fault refers to an unintended opening of a 1-phase or 2-phase conductor in an energized state. The conductor may or may not contact the ground or another medium after the open conductor fault, showing diverse aspects such as generation of arcs, maintenance of a high impedance fault (HIF), a change into a general ground fault, etc. For these reasons, power companies have traditionally experienced difficulties detecting, identifying, and coping with open conductor faults.

The associate editor coordinating the review of this manuscript and approving it for publication was Dazhong Ma.

Recent massive wildfire disasters in South Korea and US were caused by open conductor faults that were not detected by the distribution control center and protective devices [1]. Such large-scale fires degrade the reliability of the power companies' operations, and cause socioeconomic losses that jeopardize their existence. Therefore, the development of a reliable technology to detect such open conductor faults is essential for the operation of a power distribution network. Various studies have been conducted to detect open conductor faults [2]–[15]. We have classified these previous studies into three groups as follows.

First, methods were proposed that use elements that can be measured in an actual power distribution operation

or can be obtained through a simple calculation [2]–[5]. García-Santander *et al.* proposed a method to determine the faulted section through a topology analysis after detecting an open conductor using the voltage drop information of active sensors installed at the end of a distribution feeder or a lateral line [2]. Pongthavornsawad and Rungseevijitprapa proposed a detection method that uses the observation of residual current and phase angle change at the substation [3]. Jayamaha *et al.* proposed a method that sets the corrected value based on a simulation of the ratio of negative sequence current relative to the positive sequence current [4]. Wang *et al.* proposed a method using a zero sequence voltage above the open conductor point and the neutral current of the no-load transformer inside the power plant [5]. These studies successfully found the application methods according to the environment of each power company using simple measuring elements. However, methods in [2], [4], which used the voltage drop (loss) and current unbalance, have difficulty detecting when a new voltage source is maintained by the transformer connection of distributed generation (DG). The method proposed in [3] is not realistic because it is used to the absolute current phase, and the method in [5] has a difficulty because of the synchronization of measurements and the need for a no-load transformer. In all these methods, it is fundamentally difficult to distinguish open conductor fault from other events that occur in a power distribution network.

Second, methods have been proposed to detect open conductor faults and HIFs using a device to be installed on the future distribution network or a dedicated facility specially manufactured [6]–[10]. Westrom *et al.* performed an open conductor detection using a voltage drop at the position of the distribution transformer, and proposed a protection method using the transmitter and receiver of an open conductor detection signal [6]. Senger *et al.* proposed a location estimation method using communication and a detection method by the voltage unbalance measurement using a specially manufactured zero-sequence voltage sensor [7]. O'Brien *et al.* proposed a detection method that uses the simultaneous change of the voltage magnitude and angle measurement for several millisecond until it contacts the ground immediately after the open conductor using a phasor measurement unit (PMU) [8]. Vieira *et al.* discussed a method of detecting HIF through the detection of a voltage unbalance by a smart meter installed on the secondary side of a distribution transformer [9]. Adewole *et al.* proposed a method of detecting HIF when no ground fault occurs after the open conductor. Their detection method was based on a comparison between the current unbalance rate and the current prediction for a certain period in an open conductor detector [10]. These methods can be problematic in actual application owing to the economic problem in terms of the installation of additional devices in addition to the devices of the current power distribution network, and the utilization problem of the installed devices. Moreover, with these studies, there are questions about the possibility of distinguishing open conductor fault with other events with only a few fragmentary measurement factors and the possibility of open conductor detection in various configurations of distribution networks.

Third, detection methods using waveform analysis and analytical methodology have been proposed [11]–[15]. Benner and Russell proposed a method of making an assessment by configuring an expert system using the changes in the magnitude of harmonic and non-harmonic signals of phase and neutral lines [11]. Lima *et al.* proposed a method of detecting HIFs of power distribution systems based on the phase angle monitoring of third harmonics in a single measuring device [12]. Ledesma *et al.* proposed an HIF detection system through artificial neural network (ANN) learning using PMU measurement data of the normally open point and data obtained through an analysis of the situations of power distribution networks that can be assumed [13]. Guo *et al.* proposed a deep-learning-based ground fault detection method that uses the continuous wavelet transform and convolution neural network methods [14]. In addition, Gu *et al.* developed a feeder terminal unit that can judge HIFs by inputting a wavelet transform value for zero sequence current into a pre-trained neural network structure [15]. In the application of these methods to actual power distribution operations, depending on the target system, a problem arises because it is required to relearn the artificial intelligence structure, generate a huge amount of learning data, and adjust the judgment criteria of the waveform analysis methods.

In this study, we proposed a method of detecting open conductor faults in power distribution networks with DGs. The proposed method is based on the measurements of feeder remote terminal unit (RTU) that is installed for the operation of a modern power distribution network. Feeder RTUs are installed in protection devices, remote control switches, and other controllers to protect and monitor the distribution system. RTUs are commonly used in downtown areas in Europe and North America, and East Asia (e.g., Japan, Korea, and Taiwan). For their application in open conductor detection, the characteristics of open conductor faults based on RTU measurements were analyzed considering various power distribution network elements such as the fault type and fault path medium, transformer connection and iron core structure, and the number and capacity of loads and DG. Based on the analyzed characteristics, we proposed the flowchart for detecting open conductors using the open fault conditions (OFCs) of the RTUs. Using the proposed detection method, we derived three results of open conductor alarm (confidence), open conductor warning (suspicion), and no detection. Case studies using Matlab Simulink for a standardized power distribution network confirmed a higher open conductor detection rate of the proposed method compare to conventional methods that use only simple factors. We also demonstrated the excellent ability of the proposed method to perform open conductor detection by distinguishing the general events of power distribution networks. In addition, we derived the optimal detection criteria by performing a

sensitivity analysis of the target system, thus showing the applicability of the proposed method to typical power distribution networks.

II. EXTRACTION OF CHARACTERISTICS OF OPEN CONDUCTOR FAULTS IN POWER DISTRIBUTION NETWORK

A. EXTRACTIONS OF OPEN FAULTS CHARACTERISTICS BY EXPERIMENTS

Traditionally, power distribution networks apply the overcurrent protection for the detection and removal of faults, which are generally classified as shunt and series faults [16]. A shunt fault indicates a condition where a conductor directly or indirectly contacts the ground or a short circuit between conductors. A series fault refers to an asymmetric circuit where part (1- or 2-phase) of the conductor is open under energized. According to EPRI report, the majority of the distribution system faults are single phase (79%), out of which, a large percentage (19%) involve open conductor fault. As a result, about 6% of all the power distribution system faults are open conductor faults that cannot be detected by the conventional overcurrent protection system [6].

Artificial open conductor faults were experimented in the Gochang PTC (power testing center) of the KEPCO [17]. The Gochang PTC has a real high-voltage power distribution network, and receives 22.9kV from a substation, but no load is connected to it. For this experiment, a single branch line in the middle of the line was downed to the ground after open conductor and its behaviors were analyzed. For ground contact media, asphalt, gravel, soil, reinforced concrete, concrete (sidewalk block), sand, and trees were used Photos of the experimental setup and experiments were as shown in Figure 1.

(a) Installation of equipment for experiments

(b) Arc generation during an experiment ((left) dry asphalt, (right) wet sand)

FIGURE 1. Photographs for open conductor fault experiments.

The experiment results were as summarized in Table 1. As shown in this table, an arc was generated mostly when the wire made direct contact, but no arc was generated when the sheath made contact. Furthermore, in the case of reinforced concrete (like a concrete pole), the occurrence of an overcurrent was observed. Through the experiments, we observed a very large impedance (at least 0.5–400kΩ) at the open conductor point. By the results of previous empirical experiments and previous studies, this study distinguished the modes of open conductor faults, as shown in Figure 2.

TABLE 1. HIF experiment result in GoChang PTC.

Contact Material	Electric Phenomena	
	Contact with conductor	Contact with insulation sheath
Asphalt	Dry (None), Wet (Arc, 21A)	None (Damage to the sheath can cause arcing)
Gravel	Dry (None), Wet (Arc, 15A)	
Soil	Dry (Arc, 10A), Wet (Arc, 13A)	
Reinforced concrete	Dry/Wet (Overcurrent, > 100A)	
Concrete (Sidewalk block)	Dry (Arc, 15A), Wet (Arc, 15A)	
Sand	Dry (Arc, 5~12A), Wet (Arc, 10A)	
Tree	Dry (Arc, 0.84A), Wet (Arc, 24A)	

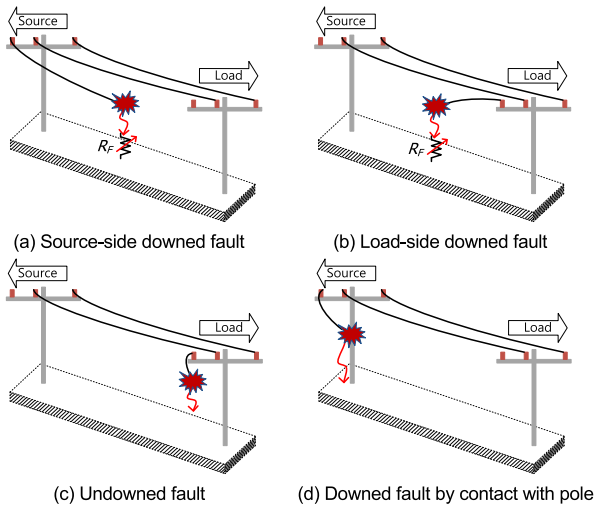

FIGURE 2. Modes of open conductor fault.

In Figure 2, the open conductor faults can be classified as 1) source-side downed fault after open conductor, 2) load-side downed fault after open conductor, 3) undowned fault after open conductor, and 4) downed fault by contact with pole after open conductor. First, for the case of source-side and load-side downed fault after open conductor, and undowned fault after open conductor, the path of fault involves a high impedance. Hence, unlike general ground faults, an accident load rejection is experienced at the source-side RTU

of the open conductor point, and at the load-side RTU of the open conductor point, the behavior immediately after open conductor is determined depending on the existence of voltage or current source. Second, the source-side downed fault by contact with pole after open conductor can show different behaviors depending on the type of the contacted pole. As shown in Table 1, in the case of a tree pole, the behavior is a high-resistance ground fault, and in the case of a reinforced concrete, a steel pipe pole or other conductive objects, the behavior is a low-resistance ground fault after some time (approximately less than 1s). The behavior of voltage and current during an open conductor fault can be also affected by the operation of protective devices and the grid code of DG operation. Therefore, the following are required for the open conductor detection of a power distribution network.

1) It can be difficult to detect the open conductor when the behavior is changed due to the contact with pole, the operation of protective devices and the DG operation by grid code. Therefore, it is necessary to detect an open conductor in a RTU before change of the mode.
2) The RTUs at the source-side and load-side of the open conductor point experience different measurements depending on the types of open conductor in Figure 2. Therefore, the characteristics of the measurement have to be analyzed through consideration of the network configuration, i.e., fault type, transformer wiring, and the capacity of load and DG, etc.

B. ANALYSIS OF OPEN FAULTS CHARACTERISTICS BY THE NETWORK CONFIGURATION

In the case of the RTU at the source-side of the open conductor point, two modes are possible. First, as shown in Figure 2(a), it can lead to a source-side downed fault immediately after the open conductor, but a high impedance condition is maintained by the medium of the contact point. The current is decreased due to the accident load rejection, but the voltage and impedance does not change significantly. Second, as shown in Figure 2(d), a high impedance is observed immediately after the open conductor, but a low-resistance ground fault is generated by contact with a pole (natural falling or movement by wind) after some time. In this case, the mode is changed some time from HIF to general ground fault; hence, a mode change can be avoided by a high-speed detection immediately after the open conductor. In the case of Figure 2(b) and 2(c), they show a similar behavior as a high impedance ground fault.

The change of measurement factors according to an open conductor in a RTU at the load-side of the open conductor point can be determined by a voltage source, a current source, or a load appeared below the open fault point. Previous studies investigated a voltage residual problem using the connection type of a transformer and a voltage residual problem according to the iron core structure of a no-load transformer (MOF) [5]. We summarized the voltage and current source appearance at the load-side of the phase ''A'' open fault.

1) Y_g-Y_g connection: In this case, the residual voltage V_r becomes 0 when an open conductor occurs by the grounding of the primary and secondary neutral points.
2) Y_g-Δ connection: Theoretically, if voltages V_b and V_c of the Y_g-side wiring are similar to nominal, the voltages V_{bc} and V_{ca} of the corresponding Δ-side are also nominal. Hence, there is a voltage source close to $1.0pu$, as shown in (1). However, if the transformer has its own load, a voltage drop of the open conductor phase can be caused by a healthy phase voltage drop. In case of a nearby load that supplies a current by the generated voltage source, a voltage drop is caused by the load current and transformer impedance. Table 2 shows the simulation results for voltage source generation in the event of an open conductor while changing the output of the linked DG by the Y_g-Δ transformer. In the simulation result in Table 2, a higher DG output can result into a slightly increased voltage, and the difference is insignificant.

$$\begin{aligned} V_{bc} &= V_{bn} - V_{cn}, \quad V_{ca} = V_{cn} - V_{an} \\ V_{ab} &= V_{an} - V_{bn} = -(V_{bc} + V_{ca}) \end{aligned} \tag{1}$$

where, the V_{ab}, V_{bc} and V_{ca} are the line-to-line voltage of Δ-side for a Y_g-Δ connection transformer. And the V_{an}, V_{bn} and V_{cn} are the line-to-neutral voltage for virtual point n.

3) Δ-Y_g or Δ-Δ connection and Δ connected load: If the transformer connection is primary Δ or Δ connected load, and if the source-side current of the corresponding phase in the event of open conductor is zero, a maximum voltage of $0.5pu$ is generated by the current source, as shown in (2). In case the transformer does not have its own load, the magnetizing impedance is used as the path; hence, the internal current is close to zero and no voltage is maintained. By contrast, if the transformer has its own load, the internal current has a significant value because the current flows to the load through the leakage impedance. Therefore, a voltage value smaller than $0.5pu$ is maintained.

$$\begin{aligned} I_a &= I_{ab} - I_{ca} = 0, \quad I_{ab} = I_{ca} \\ I_{bc} &= -\left(I_{ca} + I_{ab}\right), \quad I_{ab} = -0.5I_{bc} \end{aligned} \tag{2}$$

where, I_a is the line current of phase A. I_{ab}, I_{bc}, and I_{ca} are the phase current of Δ-side for a primary Δ connection transformer.

4) 3leg iron core structure of Y_g-Y_g connection: If a Y_g-Y_g transformer with a 3leg iron core structure has no load, the magnetic flux of the other phase is induced in the corresponding phase in the event of an open conductor, and a voltage close to $1.0pu$ is maintained theoretically. However, if it has an own load and a nearby load, the magnetic flow path is formed toward the load, and the induced voltage in the open conductor phase becomes very small.

TABLE 2. Simulation results for voltage generation in the event of single phase open fault of the DG linked to $Y_g - \Delta$ transformer.

Case (MVA)		Voltage after open conductor (p.u.)		
		DG Output		
		0%	50%	100%
Load (5MVA), DG (0.83MW), Linked TR (1MVA)		0.633	0.640	0.663
Load (5MVA), DG (2.5MW), Linked TR (3MVA)		0.808	0.832	0.872
Network parameter data	Line %Z/km	$Z_1(=Z_2)$ =3.47+j7.57%, Z_0 =8.71+j22.84%		
	Linked TR %Z	j6% (self MVA base)		
	Load MVA	1MVA (per load point)		
Network diagram	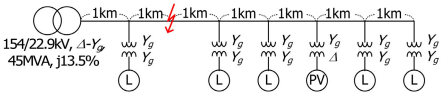			

Based on these points, the new voltage source at the load-side of the open conductor point is formulated as in (3).

$$V_r = V_{Tr}\,(\Delta) - Z_{equ(src)} \times I_{load} \tag{3}$$

where $V_{Tr}\,(\Delta)$ is the Δ winding voltage of the faulted phase induced by the healthy phase; $Z_{equ(src)}$ is the parallel equivalent of the internal impedance of voltage sources at the load-side of the open conductor point; and I_{load} is the total load current supplied by the equivalent voltage source. The current measurement of the RTU, I_{RTU} is predicted as follows:

$$I_{RTU} = \frac{Z_{down}}{Z_{up}+Z_{down}} \times \left(\frac{V_r}{Z_{equ(load)}}\right) \tag{4}$$

where $Z_{equ(load)}$ is the load equivalent impedance of loads at the load-side of the open conductor point. Z_{down} and Z_{up} are the equivalent impedances at the source-side and load-side of the RTU, respectively. The variations of the impedance measurements can be expressed as follows:

$$\Delta Z_{RTU} = \frac{\left|\frac{V_r}{I_{RTU}} - \frac{V_{pre}}{I_{pre}}\right|}{\frac{V_{pre}}{I_{pre}}} \times 100\% \tag{5}$$

where the subscript *pre* denotes the value before the open conductor fault. In addition, when an open conductor occurs, a change in the phase angle difference between the voltage and current can occur (change of current direction) at each measuring point depending on the above-mentioned voltage source and load position.

$$\begin{aligned} &|\Delta\theta_{RTU}| \le 90^\circ, \quad \textit{when there is a source above},\\ &|\Delta\theta_{RTU}| > 90^\circ, \quad \textit{when there is a source below}. \end{aligned} \tag{6}$$

where, $\Delta\theta_{RTU}$ is the measurement change in the phase angle difference between voltage and current at a RTU.

Table 3 shows the result of hand calculation using (3) to (6) and the Matlab Simulink simulation result for a simple network. We assumed a single phase open fault, with a undowned fault after the open conductor. The markings ① and ② on the network diagram denote the RTU installation positions. The network nominal voltage was assumed to be 22.9 kV, and the leakage reactance of the transformer was set to 6%. As a result, in Case 1, the voltage below the open conductor point was calculated using (3) as $V_{①} = -(0.887\angle -93.5^\circ + 1.04\angle 141.7^\circ) - 22\angle 9.12^\circ \times 26.58\angle 80.5^\circ = 0.891\angle 12.7^\circ pu$. The current measured in RTU ① is calculated as $I_{①} = \frac{5227}{5227} \times \frac{V_{①}}{5227} = 22.5\angle 12.7^\circ A$. The phase difference here is calculated as $\theta_{①} = 0^\circ$. In Case 2, there are parallel voltage sources at the load-side of the open conductor point. Compared to Case 1, the magnitude of the transformer equivalent impedance is smaller than the one of the voltage source (Y_g-Δ); hence, a voltage in the network after an open conductor larger than that in Case 1 is maintained. In Case 3, the current is distributed by the ratio of the load impedances at the source and load-side of the voltage source. Here, the RTU ① at the source-side of the voltage source experiences a reverse flow. These prove that the change of measurement factors by the RTU below the open conductor point are significantly affected by the generation of an equivalent voltage source, and the change elements can be estimated systematically.

III. ANALYSIS OF PREVIOUS OPEN CONDUCTOR FAULT DETECTION METHODS USING SIMPLE MEASUREMENT ELEMENTS

In this section, we analyzed the problems of the detection methods using the RTU measurements from previous studies that are similar to the proposed method. Previous studies that focused on open conductor detection based on RTU measurements can be classified into three categories. Method 1 involves using a voltage outage (loss) measured at a RTU and determines an open conductor if the voltage is lower than 70% of rated voltage [2]. This method can be expressed as follows:

$$\Delta V_{d,pu} = \frac{|V_d - V_{d0}|}{V_{d0}} \tag{7}$$

where V_d and V_{d0} are the voltage measurement after and before a fault, respectively. Method 2 uses the current unbalance, which occurs at an open conductor [4]. The detection method by the ratio of the positive sequence current to the negative sequence current was presented, and 15% was used as the detection criterion. For method 3, the use of the voltage unbalance rate was proposed [9]. For the calculation of the unbalance rate, this method used (8) and (9) based on the detection setting of a 30% unbalance rate:

$$K\% = \sqrt{\frac{1-\sqrt{3-6\beta}}{1+\sqrt{3-6\beta}}} \tag{8}$$

$$\beta = \frac{V_{AB}^4 + V_{BC}^4 + V_{CA}^4}{\left(V_{AB}^2 + V_{BC}^2 + V_{CA}^2\right)^2} \tag{9}$$

where $K\%$ is the voltage unbalance rate, and V_{AB}, V_{BC}, and V_{CA} are the magnitude of the line voltage.

TABLE 3. Measurement variations at the load side of the open conductor point.

Classification	Case 1	Case 2	Case 3
Calculation results	$V_{①} = 0.891\angle 12.7°pu$	$V_{①} = 0.903\angle 13.8°pu$	$V_{②} = 0.885\angle 12°pu$
	$I_{①} = 22.5\angle 12.7°A$	$I_{①} = 22.8\angle 13.8°A$	$I_{①} = 2.23\angle -168°A$, $I_{③} = 22.4\angle -12°$
	$\theta_{①} = 0°$	$\theta_{①} = 0°$	$\theta_{①} = -180°, \theta_{③} = 0°$
	$\Delta Z_{①} = -2\%$	$\Delta Z_{①} = -2\%$	$\Delta Z_{①} = 1864\%, \Delta Z_{③} = -2\%$
Matlab simulation results	$V_{①} = 0.889\angle 12.7°pu$	$V_{①} = 0.905\angle 14.8°pu$	$V_{②} = 0.883\angle 12°pu$
	$I_{①} = 22\angle 9.1°A$	$I_{①} = 22.4\angle 11.1°A$	$I_{①} = 2.21\angle -169.2°A$, $I_{③} = 21.87\angle 8.36°A$
	$① = 3.6°$	$\theta_{①} = 3.7°$	$\theta_{①} = -178.8°, \theta_{③} = 3.64°$
	$\Delta Z_{①} = -0.013\%$	$\Delta Z_{①} = -0.014\%$	$\Delta Z_{①} = 1885\%, \Delta Z_{③} = -0.01\%$
Test network	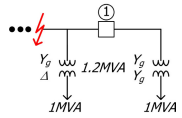	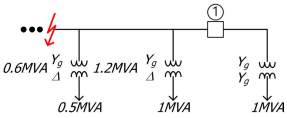	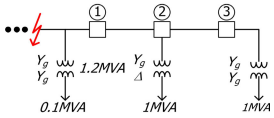

TABLE 4. Result of open conductor detection using single factor.

M	P	Cases for successful detection		Cases for detection error
		Undowned fault after open conductor	Single phase-to-ground fault	Undowned fault after open conductor
1	②	$\Delta V_{d,pu} = \frac{0.992 - 0}{0.992} = 1$ $\therefore \Delta V_{d,pu} > \Delta V_{threshold}(0.3pu)$	$\Delta V_{d,pu} = \frac{0.992 - 0}{0.992} = 1$ $\therefore \Delta V_{d,pu} > \Delta V_{threshold}(0.3pu)$	$\Delta V_{d,pu} = \frac{0.992 - 0.878}{0.992} = 0.11$ $\therefore \Delta V_{d,pu} < \Delta V_{threshold}(0.3pu)$
2	①	$\frac{I_2}{I_1}(\%) = \frac{5.5}{19} \times 100 = 29.2\%$ $\therefore \frac{I_2}{I_1}(\%) > I_{unblanced}(15\%)$	$\frac{I_2}{I_1}(\%) = \frac{8.2}{16.4} \times 100 = 50\%$ $\therefore \frac{I_2}{I_1}(\%) > I_{unblanced}(15\%)$	$\frac{I_2}{I_1}(\%) = \frac{2.1}{23.4} \times 100 = 9.2\%$ $\therefore \frac{I_2}{I_1}(\%) < I_{unblanced}(15\%)$
3	②	$\beta = 0.39$ $K\% = 29.2\%$ $\therefore K\% > V_{unblanced}(30\%)$	$\beta = 0.44$ $K\% = 50\%$ $\therefore K\% > V_{unblanced}(30\%)$	$\beta = 0.34$ $K\% = 9.2\%$ $\therefore K\% < V_{unblanced}(30\%)$
Network		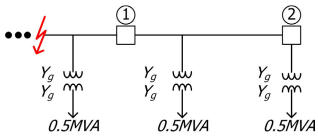		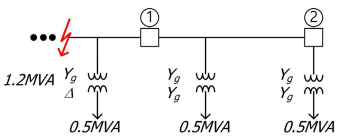

Table 4 shows the results obtained after reviewing the problems of each method mentioned above for a simple distribution networks. The marking M in Table 4 denotes the three previous research methods, and ① and ② in column P denote the positions of the RTU in the test network. The detection results of each method were examined based on the measurements at these positions. The network data used in this review were: the main transformer impedance was 30% (100MVA base), and the individual capacity of the linked transformer was 1.2MVA; the impedance was 6% (self-capacity base). Furthermore, the total line length was 5km, and the ACSR 160mm^2 data were used for the line impedance. The open conductor fault occurred at 3km. We assumed that the load capacity at the source-side of the open conductor point is 2MVA. As shown in Table 4, some problems of the conventional methods were founded. The most serious and common problem associated with these methods is that it is impossible to identify events other than open conductor (e.g., ground fault, accident load rejection), as seen in comparison with the results of the first (undowned fault after open conductor) and second column (single phase-to-ground fault) of the table. This means that the occurrence of an event may be detected but not specified, and it may be difficult to take action after the event has occurred. Moreover, as seen in the third column, when the voltage source is at the load-side of the open conductor point, there are cases where the criteria of each method are not satisfied owing to the maintenance of voltage, current flow to the load, and the reduction of voltage and current unbalances. Consequently, depending on the network configuration, it can be difficult to apply methods using single detection factor of a RTU.

IV. PROPOSAL OF OPEN CONDUCTOR FAULT DETECTION METHOD

The basic rules for proposed open conductor detection can be summarized as follows.

First, in the case of shunt faults such as general single phase-to-ground faults, the RTU at the source-side of the faulted point experiences the current increase and the voltage decrease, thus decreasing the overall impedance. In a fault situation immediately after the open conductor, an accident load rejection phenomenon occurs; thus, the current decreases while the impedance increases. If the open fault is transformed into a low-resistance ground fault upon contact with a pole, it may be difficult for the source-side instrument to distinguish it from a single phase-to-ground fault. However, some time is required until mode change. We attempted to solve such a problem of mode change by using few cycles of data before and after event detection, from event detection until the determination of the open conductor.

Second, in the case of RTU at the load-side of the open conductor point, various conditions can occur depending on whether there is a voltage or current source below the open conductor point. Representative detection factors can include a voltage outage (voltage below a certain magnitude is maintained), current outage, reverse flow phenomenon, and variations of current and impedance. Furthermore, an overvoltage phenomenon can occur if the load is smaller than the power generated by DG in the load-side network of the open conductor point.

Figure 3 shows the open conductor detection flowchart using multivariate detection factors proposed in this study. For the triggering (Step 2) and final decision (Step 3) of the open faults, we introduce the open fault condition (OFC) that is reflected above basic rules.

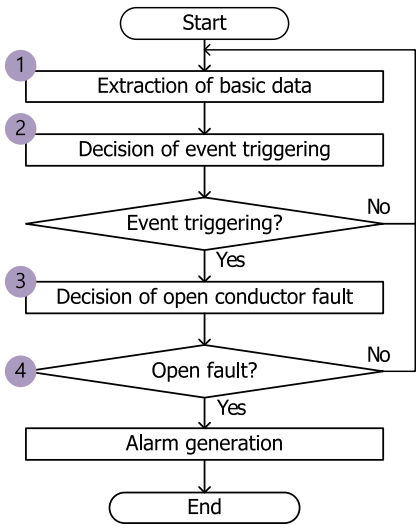

FIGURE 3. Overall flowchart for open conductor fault detection method.

[Step ①] *Extraction of Basic Data:* Each RTU in the network obtains the voltage and current waveform using a potential transformer (PT) and a current transformer (CT), and extracts the RMS values per cycle through signal processing then the current (t_0) data are stored for event detection.

[Step ②] *Decision of Event Triggering:* The factor required for event triggering is calculated by comparing the stored data, t_0, with the data at a specific time in the past (t_{-x}). If this value satisfies one or more conditions in Table 5, progress to the next step for a decision about the open conductor fault; otherwise, return to Step ①. The event triggering factors in Table 5 were set to detect most events (e.g., open conductor, ground fault, and load rejection) that occur in the distribution network. These factors were composed of overvoltage (OFC_1, V_{OV}), voltage outage (OFC_2, V_{OT}), current outage (OFC_3, I_{OT}), impedance measurement change (OFC_4, ΔZ), and change of current unbalance (ΔI_{UB}).

TABLE 5. Event triggering condition.

Event triggering factor	Detection value setting
Overvoltage (OFC_1)	$V_{OV} > V_{OV\_Ref}$
Voltage outage (OFC_2)	$V_{OT} > V_{OT\_Ref}$
Current outage (OFC_3)	$I_{OT} > I_{OT\_Ref}$
Change of impedance measurement (OFC_4)	$\Delta Z > \Delta Z_{Ref}$
Change of current unbalance	$\Delta I_{UB} > \Delta I_{UB\_Ref}$

[Step ③] *Decision of Open Conductor Fault:* When the event triggering condition is satisfied in Step ②, a decision is made about the open conductor fault. To this end, a current change due to an event (OFC_5, $|\Delta I| > \Delta I_{Ref}$) and the phase angle difference change due to reverse flow (OFC_6, $\Delta\theta > 90^o$) are used in addition to open fault conditions in Table 5. A current unbalance is not used when distinguishing an open conductor fault because it is difficult to distinguish its characteristics that occur in almost every event. $OFC_1 \sim OFC_6$ data are calculated by making a comparison between the two time points using the data (t_{-x}) stored at a specific past point ($-x$ cycle) used in the decision of event triggering, and the data (t_{+x}) of the $+x$ cycle. Figure 4 illustrates the detailed flowchart for the decision of the open conductor.

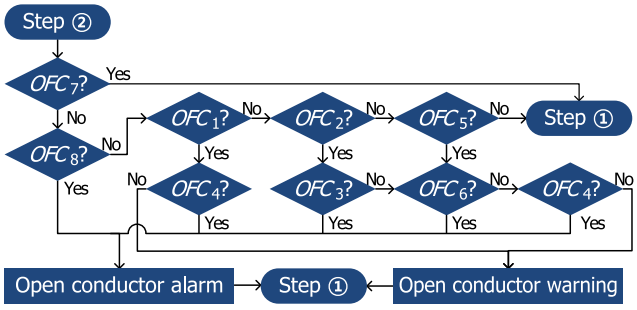

FIGURE 4. Flowchart for decision of open conductor fault.

In the case of the RTU at the source-side of the open conductor point, the general shunt fault is filtered by setting the top leftmost item in the flowchart. To distinguish the general shunt faults, the increase of current and the decrease of the

voltage due to general phase-to-ground fault was denoted by OFC_7, and the decrease of current and the maintenance of the voltage due to accident load rejection in the event of an open conductor was denoted by OFC_8.

In the case of the RTU at the load-side of the open conductor point, first, an open conductor fault is determined when an overvoltage occurs below the open conductor point through OFC_1. OFC_1 assumes a case whereby the DG output is very large relative to the load, thereby increasing the voltage. Second, if both OFC_2 and OFC_3 are satisfied, it is determined to be an open conductor fault. This used the characteristic that both the voltage and current undergo an outage because the source disappears at the load-side of the open conductor point. Finally, as mentioned in Section II, a new voltage or current source is generated at the load-side of the open conductor point due to the transformer connection. Unlike the above two cases, this varies by network configuration such as the open conductor point, load impedance ratio at the source-side and load-side of the RTU, and the position of voltage/current source. Hence, the open conductor fault was distinguished through the rules using multivariate factors. For example, if a load current at the source-side of the RTU is supplied by the new voltage source at the load-side of the RTU, the open conductor fault can be distinguished by combining the change of current direction (OFC_6) and additional factor ($OFC_2 or OFC_5$). The overall combination is indicated from the OFC_2 factor to the bottom right of Figure 4.

We classified three types of final open conductor decision into ''open conductor alarm (confidence)'', ''open conductor warning (suspicion)'', and ''no detection''. The open conductor alarm is generated when the following conditions are satisfied, two or more open conductor fault detection factors or the instrument above a fault and when there is confidence about the detection of an open conductor fault. This signal can be used by the operator or operation system to block the reclosing behavior of protective devices, and to immediately deploy field workers to reduce secondary damage by an open conductor. In the case of an open conductor warning, the event triggering factors changed significantly along with the voltage and current of the network among the open conductor fault triggering factors. However, since the additional measurement factors are not changed by the network configuration and measurement position, the open conductor based on the RTU cannot be determined; implying that the operator needs to make a decision using additional information about the assessed result of other RTUs or to consider site patrol by field workers.

V. CASE STUDY

The proposed open conductor fault detection method was verified through case studies using Matlab Simulink. Figure 5 shows the single-line diagram of the test system. For the configuration of the test system, we used the statistics of KEPCO, the only power company in South Korea [18]. The topology of the test network was composed of three feeders, and was assumed to be composed of overhead lines only.

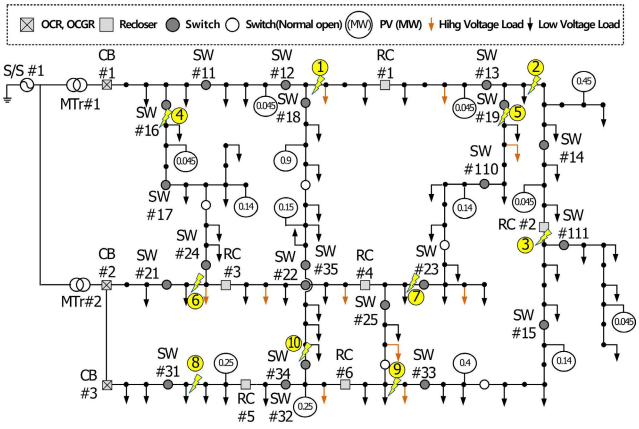

FIGURE 5. Network topology for the test of the proposed method.

Feeder 1 is a mid-to long-distance line with a total length of 24 km, composed of many PVs and a small number of high-voltage consumers. Feeder 2 and Feeder 3 are short-distance lines with a total length of 9 km. Feeder 2 only has loads (low-voltage and high-voltage loads), whereas for Feeder 3, a small number of high-voltage consumers and DGs. We assumed the reinforced concrete pole generally used in South Korea.

Each component of the test network is briefly explained below.

1) Line: We applied ACSR 160/90mm^2, which is used in high-voltage distribution feeders, using positive and negative sequences ($Z_1 = Z_2 = 3.47 + j7.57\%$) and a zero sequence ($Z_0 = 8.71 + j22.84\%$). The length of each section was set to 0.3 km.
2) Fault positions: These were marked as ①∼⑩ as shown in the test network diagram. At these positions, the open conductor fault and other events were simulated.
3) DG: The capacity of the DG connected to Feeders 1 and 3 was composed using the average DG capacity statistics by feeder length of KEPCO shown in Table 15 of the Appendix [19]. For Feeder 1, approximately 2 MVA was applied for the DG linked capacity, and for Feeder 3, 1.1 MVA was applied for the DG. Regarding the DG-linked transformer, we selected a transformer capacity that is closest to the DG capacity using the transformer catalogue of LS Electric, and the capacities are listed in Table 6 [20].
4) Transformer and load: For the wiring of the receiving transformer for high-voltage consumers in the test network, we used Δ-Y_g connection that accounts for the majority of the statistical data of Korea shown in Table 16 of the Appendix [21]. For the connection of the pole/pad-mounted transformer (for low-voltage consumers), we applied Y_g-Y_g. Regarding the total load for each feeder during simulation, we applied 5.9MVA was applied to Feeder 1, 5.48MVA to Feeder 2, and 5MVA to Feeder 3. The individual loads applied in the test network were as defined in Table 6.

TABLE 6. Load and DG-linked transformer for the test network.

Feeder		Load-linked TR		PV-linked TR		
		Connection (MVA)	Load MVA (Number)	Wiring	TR MVA	PV MW (Number)
1	LV	Y_g-Y_g (0.3)	0.15 (30)	Y_g- Δ	0.2	0.045(5)
					0.2	0.14(3)
	HV	Δ-Y_g (1.0)	0.35(2)		0.6	0.45(1)
			0.7(1)		1.0	0.9(1)
2	LV	Y_g-Y_g (0.3)	0.19 (12)	Y_g- Δ	No connected PV	
	HV	Δ-Y_g (1.0)	0.55(2)			
			0.7(3)			
3	LV	Y_g-Y_g (0.3)	0.2 (16)	Y_g- Δ	0.3	0.15(1)
					0.3	0.25(2)
	HV	Δ-Y_g (1.0)	0.9 (2)		0.5	0.4(1)

5) Application of grid code: For simulations similar to the actual power distribution network, we applied the grid code standard of Korea shown in Table 17 of the Appendix to the PV inverters used in the test system [22].
6) Protective devices: To verify the open conductor detection problem according to the operation of protective devices, we applied three protective devices to each feeder, as shown in Figure 5. We installed circuit breaker (CB) based on an overcurrent relay at the start point of the feeder, and a recloser in the middle of the distribution line. The coordination time interval (CTI) between the relay of the feeder starting point CB and recloser was set to 10 cycles, and the CTI between reclosers to 5 cycles [23], [24]. In addition, we considered a protection coordination according to the sequence coordination function for operation cooperation between reclosers 24].
7) RTU: RTUs are installed in the protection device and switch in Figure 5 to verify the proposed method. RTUs measure 1-cycle data (e.g., voltage, current magnitude, phase angle difference) using 128 samples of data per cycle through the CT and PT installed at the corresponding points. Therefore, this study determined the detection of open conductor faults by extracting 1-cycle data obtained from Matlab Simulink for similar simulations. For the decision of open conductor fault in Fig. 4, we assumed the time of t_{+x} to be 5cycles for considering the trip time of protective devices.
8) Fault type: The fault types listed in Table 7 were simulated at each fault position on the test network. Among the open conductor faults, when there is contact with the pole (reinforced concrete pole) after the open conductor, such as Types 2 and 4, few times are required by falling until the disconnected line comes into contact with the support. Therefore, we simulated it to change from high-resistance immediately after the open conductor to low-resistance (contact with support) in approximately 1s. Furthermore, in the case of a ground fault, the ground fault resistance of each fault was simulated by classifying the faults as low-resistance (Type 11) and high-resistance (Type 12). Therefore, a total of 19 fault types were applied in the simulation. With respect to the load rejection, a load rejection of the load-side that is closest to the fault position was simulated.

TABLE 7. Fault simulation cases.

Type	Event
Type1	Source-side downed fault after 1phase open fault (2,000Ω)
Type2	Contact with source-side pole after 1phase open fault (2,000Ω→30Ω)
Type3	Load-side downed fault after 1phase open fault (2,000Ω)
Type4	Contact with load-side pole after 1phase open fault (2,000Ω→30Ω)
Type5	Undowned fault after 1phase open fault
Type6	Source-side downed fault after 2phase open fault (2,000Ω)
Type7	Contact with source-side pole after 2phase open fault (2,000Ω→30Ω)
Type8	Load-side downed fault after 2phase open fault (2,000Ω)
Type9	Contact with load-side pole after 2phase open fault (2,000Ω→30Ω)
Type10	Undowned after 2phase open fault
Type11	Low-resistance 1phase-to-ground fault (3, 5, 15, 30Ω)
Type12	High-resistance 1phase-to-ground fault (50, 100, 1,000Ω)
Type13	High-voltage load rejection
Type14	Low-voltage load rejection

A. COMPARISON BETWEEN PROPOSED METHOD AND CONVENTIONAL METHODS

We compared the proposed method with three existing methods mentioned in Section III for Feeder 3 in Figure 5. 56 faults were simulated by changing 19 fault types and 3 fault positions. The number of RTUs for Feeder 3 was 8, but different target number of event decision were derived because of differences in the RTU positions assessed by each method. For example, in the case of the proposed method and Method 2, when faults are generated at a fault position ⑧, 152 cases are derived (19 fault types × 8 RTUs = 152). However, RTU SW#34 and SW#35, which existed on the lateral branch lines when an event occurred at fault position ⑨, were excluded from the total case because they are not related to the event detection. In the case of fault position ⑧ of Methods 1 and 3, it is evaluated only to the load-side of the open point, applied 38 cases were derived (19 fault types × 2 RTUs = 38).

The open conductor detection rate for each method was analyzed using two indices. The first is the "*total detection rate*," which is an index that indicates whether an open conductor and other events (ground fault or accident load rejection) were accurately detected in all events defined in Table 7. The second is the "*open conductor detection rate*," which is a detection index that focuses on open conductor faults. The detection criteria of the above-mentioned *OFC* were set as shown in Table 8.

The simulation results were as summarized in Tables 9 and 10. In these tables, "A/B" denotes the "number

TABLE 8. Detection criteria of the proposed method.

Classification	Settings
OFC_1	$V_{OV} > 120\%$
OFC_2	$V_{OT} > 50\%$
OFC_3	$I_{OT} > 50\%$
OFC_4	$\|\Delta Z\| > 20\%$
OFC_5	$\|\Delta I\| > 20\%$
OFC_6	$\|\Delta\theta\| > 90^o$
OFC_7	$\Delta I > 20\%$
OFC_8	$\Delta I < -20\%$

TABLE 9. Open conductor detection rate for feeder 3.

Method	Fault position			Detection rate
	⑧	⑨	⑩	
Proposed Method	80/80 (100%)	56/60 (93.3%)	52/60 (86.7%)	94%
Method 1	10/20 (50%)	5/10 (50%)	10/10 (100%)	62.5%
Method 2	80/80 (100%)	32/60 (53.3%)	29/60 (48.3%)	70.1%
Method 3	10/20 (50%)	5/10 (50%)	5/10 (50%)	50%

TABLE 10. Total detection rate for feeder 3.

Method	Fault position			Detection rate
	⑧	⑨	⑩	
Proposed Method	127/152 (83.5%)	96/114 (84.2%)	91/108 (84.3%)	84%
Method 1	28/38 (73.6%)	11/19 (57.9%)	17/18 (94.4%)	74.7%
Method 2	127/152 (83.5%)	59/114 (51.8%)	45/108 (41.6%)	61.8%
Method 3	28/38 (73.6%)	13/19 (68.4%)	13/18 (72.2%)	72%

of accurate decisions/target number of decisions''. As shown in Table 9, as a result of the simulation of method 1, most open conductor faults were detected when the impact of DG was small, such as fault position ⑩. However, the open conductor detection rate decreased as the impact of the DG increased, as with fault positions ⑧ and ⑨. As a result of method 2 using a current unbalance, open conductor faults that occur near the feeder starting point, such as fault position ⑧, are easily detected because there is a large load that is rejected. However, in fault positions ⑨ and ⑩, the detection rate decreased significantly, and detection failed in a specific section due to a newly generated voltage source. In the case of method 1 and method 3, the detection rate was low due to the newly created voltage source. In general, the detection rate of the conventional methods was lower than that of the proposed method.

Table 10 shows the accurate open conductor detection rates for all event types. The proposed method shows a much higher detection rate compared to the conventional methods, except at fault position ⑩, which is not influenced by the DG, implying that the proposed method can distinguish not only whether or not an event occurred, but also which event occurred. In other words, the conventional methods can detect the occurrence of events, but they are unable to identify them. This is a critical feature that significantly impacts the follow-up action of the operator after event detection.

Figure 6 shows the detection result of the proposed method at the source-side (SW#32) and load-side (SW#35) of the open conductor point when a type 5 fault occurred at fault position ⑩.

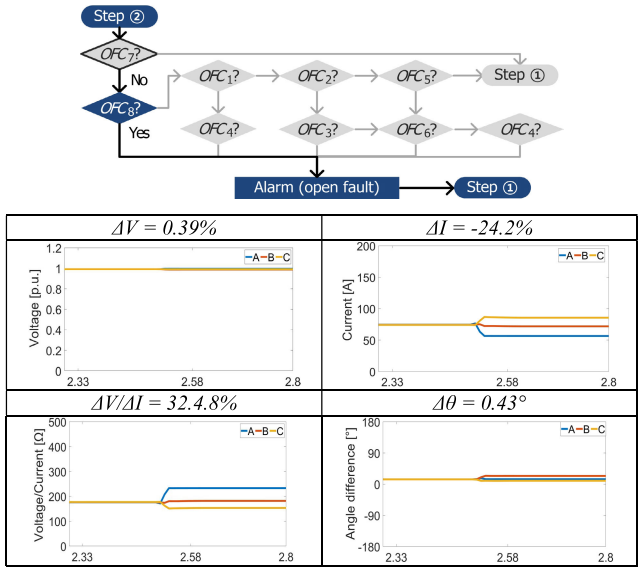

(a) Detection result at the source-side of the open conductor point (SW#32)

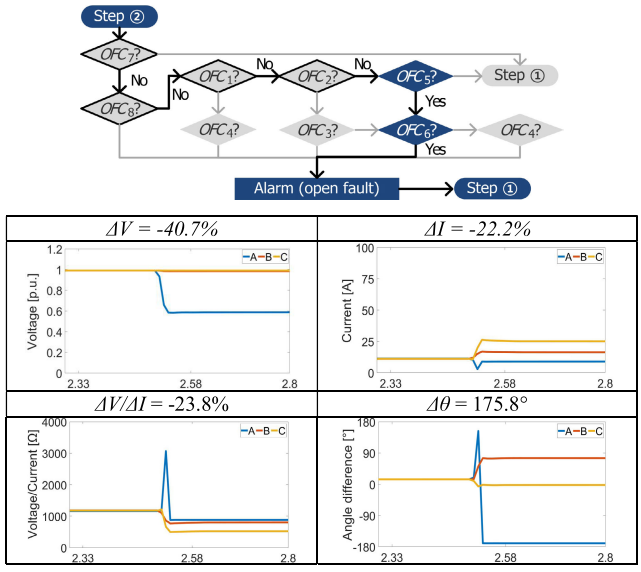

(b) Detection result at the load-side of the open conductor point (SW#35)

FIGURE 6. Detection of open conductor fault for type 5 at fault point ⑩.

Using the proposed method, the RTU at the source-side of the open conductor point detects the fault as an open conductor alarm by OFC_8, whereas the RTU at the load-side of

the open conductor point detects the fault due to reverse flow from a newly generated voltage source by OFC_5 and OFC_6. In addition, both the RTUs at the source-side and load-side of the open conductor point detect the open conductor.

Figure 7 shows the detection results of the type 11 low-resistance ground fault at the source-side (SW#32) and load-side (SW#33) of the fault point ⑨. As shown in Figure 7(a), the RTU at the source-side of the fault point satisfies OFC_7 by increasing the fault current, and thus no alarm is generated However, the RTU at the load-side of the fault point satisfies OFC_4 and OFC_5 by the fault current, and this can cause an open conductor judgement error of the RTU.

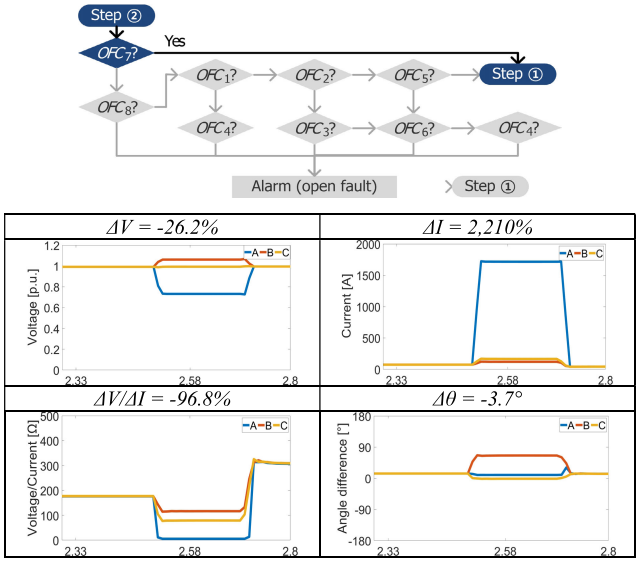

(a) Detection result at the source-side of the open conductor point (SW#32)

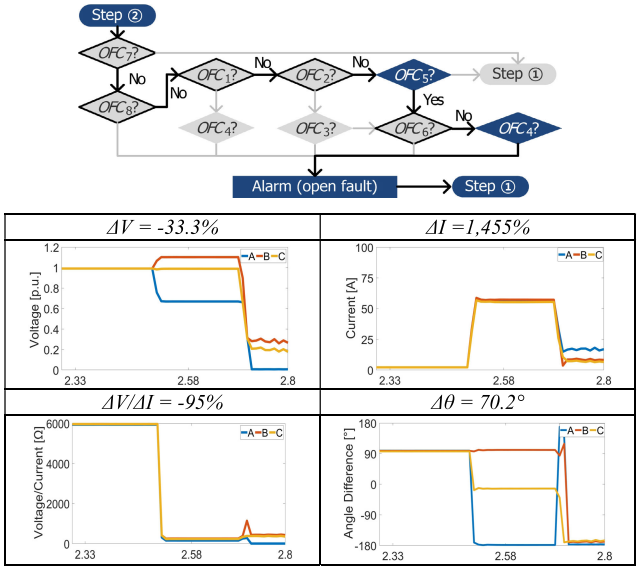

(b) Detection result at the load-side of the open conductor point (SW#33)

FIGURE 7. Detection of open conductor fault for type 11 at fault point ⑨.

However, if a low-resistance ground fault occurs owing to contact with the pole after the open conductor, such as a type 2 fault at the same position, all RTUs at the source-side and load-side of the open conductor before contact with the pole will classify it as an open conductor, when the proposed method is used, as shown in Figure 8(a) and 8(b).

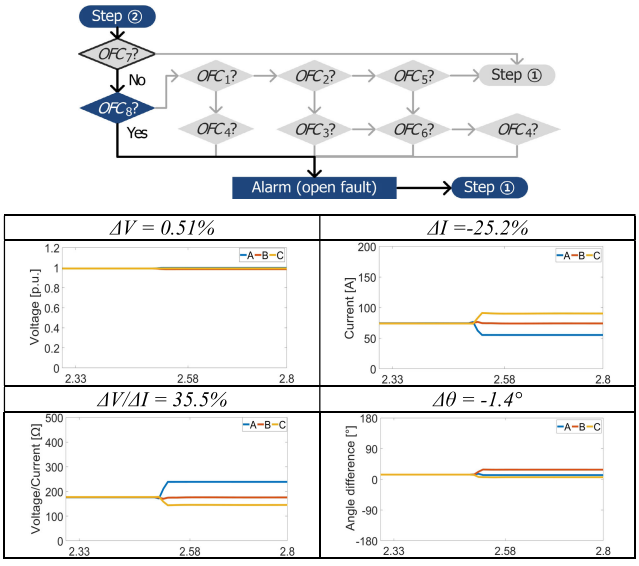

(a) Detection result at the source-side of the open conductor point (SW#32)

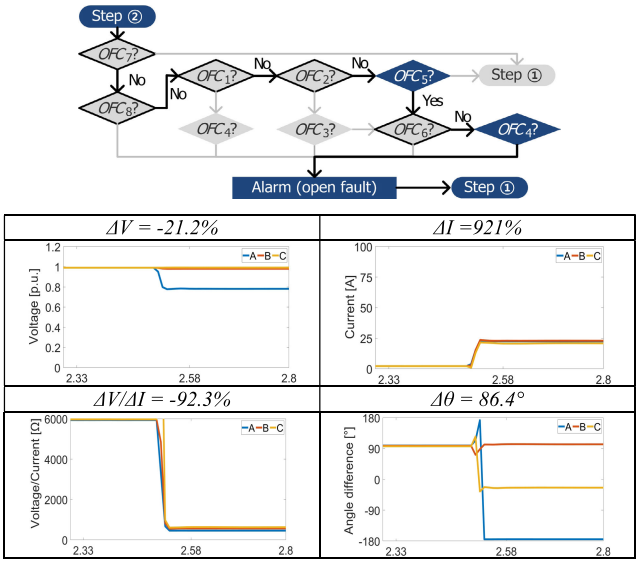

(b) Detection result at the load-side of the open conductor point (SW#33)

FIGURE 8. Detection of open conductor fault for type 2 at fault point ⑨.

The cases in Figures 7 and 8 indicate that even when the proposed method is used, if a low-resistance ground fault occurs, the open conductor fault and ground fault can be confused at the load-side RTU of the faulted point. However, the misdetection can be corrected as a ground fault by the operator through the screen information of the distribution management system (DMS) instead of the corresponding RTU. This is because RTUs at the load-side of a certain point on the screen display an open conductor alarm and the source-side protective device trips, but no RTU above

the protective device detected the open conductor. In this case, the operator can consider it as a ground fault. If the RTUs above the corresponding protective device displayed an open conductor alarm on the screen in the same situation, the operator may consider it as a contact with the pole after the open conductor.

B. RESULT OF OPEN CONDUCTOR DETECTION FOR THE ENTIRE TEST NETWORK

The total number of tests for analyzing the total detection rate is determined by multiplying the number of fault positions for each feeder, 19 fault types listed in Table 7, and the number of RTUs of the corresponding feeder. The target number of total detection rate was calculated as 1,360, and the target number of open conductor detection rate was 730.

The values in Table 8 were applied for the *OFC* threshold regarding the open conductor detection of the proposed method. To reflect the circumstance of actual operation, we analyzed the detection result of the proposed method when noise is inserted for the measurements. For the measurement noise, we inserted noise of ±3% into the voltage measurements based on the protection class 3 standard of IEEE C57.13 and IEC 61869, and noise of ±5% into the measured current [25], [26]. We conducted a random noise test by applying the standard deviation of 3σ for the noise distribution. Table 11 summarizes the test result for all feeders. The total detection rate appeared as 81∼91%, whereas the open conductor detection rate was derived as 91∼100%. As mentioned in previous section, not only the open conductor was detected, but also the open conductor detection rate for distinguishing the fault from other events was very high as well. Moreover, the fact that there is not much variation in the noise insertion and open conductor detection rate indicates the robustness of the proposed method to noises that occur in actual networks. Additionally, a test was conducted by inserting harmonics of 3%, as specified in IEEE Standard 519, into the network voltage to confirm the its effect on the proposed method when harmonics are inserted into the system [27]. The harmonic effects of the proposed method were analyzed by applying 3rd and 5th harmonics to Feeder 1 respectively, the results were as shown in Table 12. These results confirmed that the proposed method is not significantly affected by harmonics because it uses the RMS value.

TABLE 11. Detection result for all feeders.

Classification		Feeder 1	Feeder 2	Feeder 3	Detection rate
All events	Normal	595/720 (82.6%)	242/266 (91%)	314/374 (84%)	84.6%
	Noise	584/720 (81.1%)	243/266 (91.4%)	313/374 (83.6%)	83.7%
Open faults	Normal	359/390 (92.1%)	140/140 (100%)	188/200 (94%)	94.1%
	Noise	357/390 (91.5%)	140/140 (100%)	190/200 (95%)	94.1%

TABLE 12. Detection result for feeder 1.

Classification		Fault positions ①	②	③	④	⑤	Detection rate
All events	Normal	84%	86%	76%	78%	87%	82.6%
	Noise	84%	86%	76%	74%	79%	81.1%
	3rd harmonic	84%	83%	78%	74%	86%	82%
	5th harmonic	84%	83%	78%	74%	86%	82%
Open faults	Normal	100%	98%	81%	67%	97%	92.1%
	Noise	100%	98%	81%	67%	94%	91.5%
	3rd harmonic	100%	98%	87%	67%	97%	93.6%
	5th harmonic	100%	98%	87%	67%	97%	93.6%

Tables 12 to 14 show the detection result for each feeder of the proposed method. Table 12 shows the result of Feeder 1, which has the largest number and capacity of DGs among the three feeders. The total detection rate for Feeder 1 exceeded 81%, and the open conductor detection rate exceeded 91%. The open conductor misdetection cases in this feeder are as follows. First, a relatively high voltage is maintained below the open conductor owing to the larger DGs. In some line sections, there are no significant differences prior to and after an open fault. Second, as in the case of fault positions ③ and ④, if the load at the load-side of the open conductor point was small, there would be a problem in the event recognition and detection because it would be difficult to detect the change. Table 13 shows the result of Feeder 2 in which only loads exist. The proposed method has a detection rate of 92.1% and an open conductor detection rate of 100%. According to the fault mode of the open conductor in a network where only loads exist, most open conductor faults can be detected through the voltage and current outage conditions. Table 14 shows the detection rate of Feeder 3 linked with a small number of DGs. The total detection rate was 83% or higher, and the open conductor rate was 95% or higher. As a result, the effect of the new voltage source at the load-side of the open conductor point was also small. For this reason, Feeder 3 showed a higher detection rate compared to Feeder 1.

TABLE 13. Detection result for feeder 2.

Classification		Fault position ⑥	⑦	Detection rate
All events	Normal	92.7%	88.6%	91%
	Noise	93.4%	88.6%	91.4%
Open faults	Normal	100%	100%	100%
	Noise	100%	100%	100%

TABLE 14. Detection result for feeder 3.

Classification		Fault position ⑧	⑨	⑩	Detection rate
All events	Normal	83.5%	84.2%	84.3%	84%
	Noise	83.5%	83.3%	84.3%	83.7%
Open faults	Normal	100%	93.3%	86.7%	94%
	Noise	100%	95%	88.3%	95%

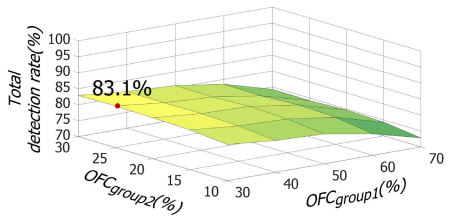

(a) Sensitivity analysis for total detection rate of Feeder 1

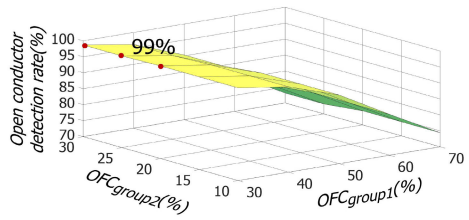

(b) Sensitivity analysis for open conductor detection rate of Feeder1

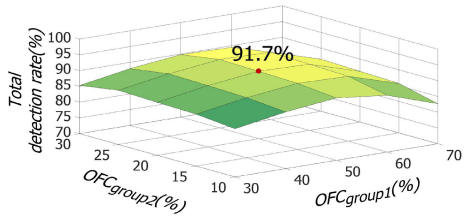

(c) Sensitivity analysis for total detection rate of Feeder 2

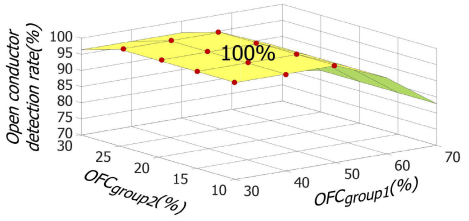

(d) Sensitivity analysis for open conductor detection rate of Feeder 2

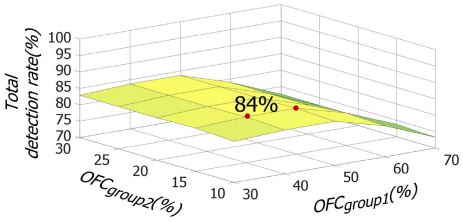

(e) Sensitivity analysis for total detection rate of Feeder 3

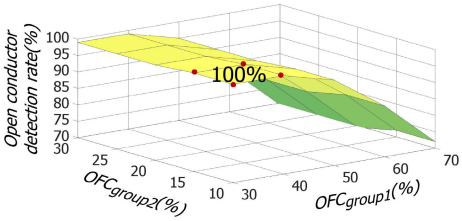

(f) Sensitivity analysis for open conductor detection rate of Feeder 3

FIGURE 9. Open conductor detection result according to different OFC settings.

C. SELECTION OF OPTIMAL OFC FACTOR THROUGH SENSITIVITY ANALYSIS

The open conductor fault detection rate was analyzed while varying the *OFC* threshold in order to determine the optimal *OFC* in the test network. For the factors included in the sensitivity analysis, the *OFC* factors were divided into two groups; $OFC_{group1}(OFC_2, OFC_3)$ based on the 50% level in Table 8 and $OFC_{group2}(OFC_4, OFC_5, OFC_7, OFC_8)$ based on the 20% level. The phase angle difference criterion OFC_6 and the overvoltage criterion OFC_1 were set to the values in Table 8. To determine the optimal *OFC* settings, the detection results were examined while simultaneously changing each setting of *OFCs* that belong to OFC_{group1} and OFC_{group2}. OFC_{group1} was tested using settings in the range of 30∼70% by changing it by ±10% from 50%. And also, OFC_{group2} was tested using settings in the range of 10∼30% by changing it by ±5% from 20%.

Figure 9 shows the sensitivity analysis result for open conductor detection according to the change in the *OFC* settings for each feeder. The X-axis represents OFC_{group2}, and the Y-axis represents OFC_{group1}; the Z-axis represents each detection rate. In each figure, the lighter color of the corresponding area represents a higher detection rate, and the darker color represent lower detection rates. The *OFC* condition from which the maximum detection rate was derived and the detection rate were as shown in each graph.

The sensitivity analysis result for *OFC* showed that in the case of a network with a large linkage capacity of DG, the more sensitive the condition of OFC_{group1}, the higher the probability of open conductor detection. This is because as the DG linkage increases, the effect of the voltage source generated at the load-side of the open conductor point becomes larger. Furthermore, as OFC_{group2} becomes more sensitive, it is more sensitive to the accident rejection of loads, when they are set higher and the fault position is closer to the end of the line, it becomes more difficult to detect an event. Hence, appropriate settings are required.

Feeder 1 showed the highest total detection rate of 83.1% when the OFC_{group1} was 30% and the OFC_{group2} was 25%. Feeder 1 is connected with many DGs, and has the largest voltage source at the load-side of the open conductor point. Therefore, lowering the outage condition at the load-side of the open conductor point increased the open conductor detection rate of Feeder 1. Feeder 2 showed the highest detection rate when the OFC_{group1} was 50% and the OFC_{group2} was 20%. In a network having only loads such as Feeder 2, making the *OFC* setting more sensitive increases the confusion rate with other events. Furthermore, if the *OFC* is set higher with an attempt to prevent this, it becomes more difficult to detect a fault located closer to the end of the line. Feeder 3 showed the highest detection rate when the OFC_{group1} was 40% and the OFC_{group2} was 15%. Since Feeder 3 has a smaller capacity of

DG linked to the network than Feeder 1. The detection rate increases if the voltage outage condition is lower than that of Feeder 1.

In conclusion, as shown by the sensitivity analysis result, the optimal *OFC* setting can differ according to the network configuration. Therefore, if the *OFC* settings for the target network are analyzed in advance using the network data of the power company (e.g., locations of terminal units, DG linkage information, and load data) before applying the proposed method to the power distribution network, it could be used as a basis for the improvement of the detection accuracy for open conductor faults.

VI. CONCLUSION

This study proposed an open conductor detection method in a power distribution network with DG. The proposed method systematically analyzed the characteristics of open conductor faults in a power distribution network. In addition, we proposed a method of increasing the open conductor fault detection rate by combining the measuring elements of the existing RTUs without additional installation of facilities and instruments. The following conclusions were made about the proposed open conductor fault detection method.

1) In comparison with the conventional methods, we verified that the proposed method increased the detection rate for open conductor faults by at least 20%. The main reason for this difference is that the conventional methods do not consider the new voltage sources that appear at the load-side of the open fault point. This is because these new voltage sources have a huge impact on the voltage, current and current direction below the faulted point. The proposed method improved the reliability of detection by using multivariate rules.
2) When open conductor faults and other events such as general ground faults were tested together, the proposed open conductor detection method showed a detection rate of approximately 84% or higher, which is at least 10% higher than the conventional methods. This means that the proposed method can not only distinguish whether an event occurred but also determine which event occurred. Nevertheless, a problem arises that an open conductor fault alarm is generated in the case of the RTU at the load-side of the fault point when low-resistance ground faults occur. However, these problems can be improved if the judgment results of individual RTUs are collected at the operating system level such as DMS, and the operator reviews the overall information including the operation status of the protective equipment. Identifying the current event is important for the operator of the operation center to determine follow-up measures, and this can be a significant advantage in the operation of a power distribution network.
3) To verify the proposed open conductor detection method, we tested it on a test network composed of three feeders. We also conducted a random noise test for application to actual power distribution systems. The random noise test result showed a difference of less than 1% in the detection rate. In addition, we confirmed that the proposed detection method was not significantly affected by the harmonic injection of the voltage measurement value. This result proved that the proposed method was highly robust to the measurement noises and harmonics that occur in actual networks. The test results for each feeder showed that the total detection rate was 81∼91% and the open conductor detection rate was 91∼100%. The detection rate decreased slightly for a feeder with a higher DG linkage capacity. This is because as the DGs linked to the network increase, the holding voltage at the load-side of the open conductor point stays close to the normal voltage making it difficult to detect faults in individual RTUs. However, this problem can be addressed by the operator by reviewing the detection results of various RTUs that applied the proposed method in this study at the operation system level. Furthermore, as mentioned in Section I, the authors did not consider additional investments in devices and infrastructure, but believe that the detection reliability can be further improved in future by the incorporation of high-precision measuring instruments that guarantee synchronization, such as a phasor measurement unit, to power distribution networks.
4) To apply the proposed method to the operations of an actual power distribution network, the method needs to be tested in various environments. To this end, a sensitivity analysis was performed for the settings of two groups of *OFCs*, and the optimal judgment criteria for the target network were derived. Thus, with respect to the open conductor misdetection problem due to the voltage maintained by a voltage source, the open conductor detection reliability for the target network increased when the sensitivity of OFC_{group1} was adjusted. In the case of a network with only loads such as Feeder 2, if the OFC_{group1} such as Feeders 1 and 3 are adjusted to be more sensitive, the probability of misdetection faults such as general ground faults increases. Furthermore, if it is adjusted to be very insensitive, there are problems with respect to event recognition and identification. Consequently, the detection rate for open conductor faults can be significantly improved by performing a preliminary analysis for the settings of detection elements before the proposed method is applied to the field using network data of the power company (e.g., locations of terminal units, DG linkage information, and load data).
5) The contributions of this study are as follows. First, the suitability of the factors used for detection in real network operations can be improved by employing the magnitudes and phase differences of the voltage and current, which are general variables that can be

measured in typical RTUs. Second, the accuracy of open conductor detection when linking a DG and the limitations on the detection being distinguished from other events that are the problems of the existing methods were improved using multivariate OFCs. Third, we demonstrated the applicability of the proposed method to a real system by deriving the optimal detection criteria using a sensitivity analysis for the target network.

6) To extend the proposed method to the fault detection tool for general purpose in the power distribution networks, additional studies in the following aspects are required. First, detection results can be improved through a comprehensive fault judgment at the operation system (DMS) level based on the detection results of individual RTUs. Second, Additional studies are required for detection of HIFs among the general shunt faults. Additionally, this method proposed an open conductor fault detection method for radial power distribution systems. In the case of the closed loop network system, a detection problem of the proposed method may occur because the characteristics of the fault are different. Therefore, a separate study is required for the looped networks.

The increasing complexity of distribution network operation resulting from the increasing linkages of DGs is a common problem worldwide. Based on the above discussion, we believe that the application of the proposed open conductor detection method for power distribution networks could be effective in the actual operation of power distribution networks.

APPENDIX

Tables 15 to 17 show the average DG capacity statistics by feeder length [19] as mentioned in Section V, the high voltage customers' transformer wiring statistics [21], and the data related to the grid code standard for PV inverters [22].

TABLE 15. The average capacity of DG according to the line length.

Total number of feeders with DG	Line length	Number of feeders	Average capacity of DG
789	0~5km	52	1,200 kVA
	5~10km	67	1,152 kVA
	10~20km	150	835 kVA
	20~30km	107	1,971 kVA
	30~40km	84	2,786 kVA
	40~50km	68	3,527 kVA
	exceed 50km	261	6,397 kVA
	Total	789	3,320 KVA

TABLE 16. Statistics of transformer connection of high voltage customers.

Range / Tr	51~100 (kW)	101~300 (kW)	301~500 (kW)	501~1000 (kW)	1001~ (kW)
Y_g-Y_g	3.2%	2.5%	2.4%	2.5%	2.6%
Δ-Y_g	**84.5%**	**89.8%**	**90.7%**	**87.5%**	**79.6%**
Y_g-Δ	5.3%	3.4%	3.4%	3.5%	3.6%
Δ- Δ	7%	4.2%	3.5%	6.5%	14.2%
Total	100%	100%	100%	100%	100%

TABLE 17. Grid code of PV inverter for network voltage ranges.

Voltage range (%)	Trip time (Sec)
$V < 50$	0.5
$50 \leq V < 70$	2.00
$70 \leq V < 90$	2.00
$110 < V < 120$	1.00
$120 \leq V$	0.16

REFERENCES

[1] G. Bade. (Nov. 2018). *PG&E Reports Second Line Fault in Camp Fire Area*. [Online]. Available: https://www.utilitydive.com/news/pge-reports-second-line-fault-in-camp-fire-area/542633/

[2] L. Garcia-Santander, P. Bastard, M. Petit, I. Gal, E. Lopez, and H. Opazo, "Down-conductor fault detection and location via a voltage based method for radial distribution networks," *IEE Proc.-Gener., Transmiss. Distrib.*, vol. 152, no. 2, pp. 180–184, Mar. 2005.

[3] A. Pongthavornsawad and W. Rungseevijitprapa, "Broken conductor detection for overhead line distribution system," in *Proc. Asia–Pacific Power Energy Eng. Conf.*, Wuhan, China, Mar. 2011, pp. 1–4.

[4] D. K. J. S. Jayamaha, I. H. N. Madhushani, R. S. S. J. Gamage, P. P. B. Tennakoon, J. R. Lucas, and U. Jayatunga, "Open conductor fault detection," in *Proc. Moratuwa Eng. Res. Conf. (MERCon)*, Moratuwa, Sri Lanka, May 2017, pp. 363–367.

[5] X. Wang, T. Ding, and W. Xu, "An open conductor condition monitoring scheme using natural voltage and current disturbances," *IEEE Trans. Power Del.*, vol. 34, no. 3, pp. 1193–1202, Jun. 2019.

[6] A. C. Westrom, A. P. S. Meliopoulos, G. J. Cokkinides, and A. H. Ayoub, "Open conductor detector system," *IEEE Trans. Power Del.*, vol. 7, no. 3, pp. 1643–1651, Jul. 1992.

[7] E. C. Senger, W. Kaiser, J. C. Santos, P. M. S. Burt, and C. V. S. Malagodi, "Broken conductors protection system using carrier communication," *IEEE Trans. Power Del.*, vol. 15, no. 2, pp. 525–530, Apr. 2000.

[8] W. O'Brien, E. Udren, K. Garg, D. Haes, and B. Sridharan, "Catching falling conductors in midair—Detecting and tripping broken distribution circuit conductors at protection speeds," in *Proc. 69th Annu. Conf. Protective Relay Eng. (CPRE)*, College Station, TX, USA, Apr. 2016, pp. 1–11.

[9] F. L. Vieira, P. H. M. Santos, and J. M. C. Filho, "A voltage-based approach for series high impedance fault detection and location in distribution systems using smart meters," *Energies*, vol. 12, no. 15, pp. 3022–3027, Aug. 2019.

[10] A. C. Adewole, A. Rajapakse, D. Ouellette, and P. Forsyth, "Residual current-based method for open phase detection in radial and multi-source power systems," *Int. J. Electr. Power Energy Syst.*, vol. 117, May 2020, Art. no. 105610.

[11] C. L. Benner and B. D. Russell, "Practical high-impedance fault detection on distribution feeders," *IEEE Trans. Ind. Appl.*, vol. 33, no. 3, pp. 635–640, May 1997.

[12] É. M. Lima, R. D. A. Coelho, N. S. D. Brito, and B. A. D. Souza, "High impedance fault detection method for distribution networks under non-linear conditions," *Int. J. Electr. Power Energy Syst.*, vol. 131, Oct. 2021, Art. no. 107041.

[13] J. J. G. Ledesma, K. B. do Nascimento, L. R. de Araujo, and D. R. R. Penido, "A two-level ANN-based method using synchronized measurements to locate high-impedance fault in distribution systems," *Electr. Power Syst. Res.*, vol. 188, Nov. 2020, Art. no. 106576.

[14] M.-F. Guo, X.-D. Zeng, D.-Y. Chen, and N.-C. Yang, "Deep-learning-based earth fault detection using continuous wavelet transform and convolutional neural network in resonant grounding distribution systems," *IEEE Sensors J.*, vol. 18, no. 3, pp. 1291–1300, Feb. 2018.

[15] J.-C. Gu, Z.-J. Huang, J.-M. Wang, L.-C. Hsu, and M.-T. Yang, "High impedance fault detection in overhead distribution feeders using a DSP-based feeder terminal unit," *IEEE Trans. Ind. Appl.*, vol. 57, no. 1, pp. 179–186, Jan. 2021.

[16] J. C. Das, *Power System Analysis: Short-Circuit Load Flow and Harmonics*. New York, NY, USA: Marcel Dekker, 2002, p. 39.

[17] Y.-B. Jung, "Development of method for detecting high impedance fault," KEPCO, Na-ju, South Korea, Tech. Rep. R11DA01, Sep. 2013, pp. 90–93.

[18] J.-H. Choi, "Design and control of next-generation active distribution network based on intelligent power equipments," KEPCO, Naju-si, South Korea, Tech. Rep. R18XA04, Jun. 2021, pp. 197–211.
[19] *Statistics of Cumulative Capacity of DG in KEPCO*, Korea Electric Power Corporation, Naju-si, South Korea, 2021.
[20] LS Electric. (Jan. 2021). *Catalog of Cast Resin Transformer*. [Online]. Available: https://www.ls-electric.com/ko/product/view/P01110
[21] *Statistics of Transformer Connection of High Voltage Customer*, Korea Electric Power Corporation, Naju-si, South Korea, 2021.
[22] *Technical Standards of the Distributed Energy Resource Connection in Power Distribution System*, KEPCO, Naju-si, South Korea, 2018.
[23] A. Samadi and R. Mohammadi Chabanloo, "Adaptive coordination of overcurrent relays in active distribution networks based on independent change of relays' setting groups," *Int. J. Electr. Power Energy Syst.*, vol. 120, Sep. 2020, Art. no. 106026.
[24] M.-G. Choi, S.-J. Ahn, J.-H. Choi, S.-M. Cho, and S.-Y. Yun, "Adaptive protection method of distribution networks using the sensitivity analysis for changed network topologies based on base network topology," *IEEE Access*, vol. 8, pp. 148169–148180, 2020.
[25] *IEEE Standard Requirements for Instrument Transformers*, Standard C57.13, 2016.
[26] *IEC Instrument Transformers—Part 2: Additional Requirements for Current Transformers*, Standard 61869, IEC, 2012.
[27] *IEEE Recommended Practice and Requirements for Harmonic Control in Electric Power System*, Standard 519, 2014.

JI-SONG HONG (Graduate Student Member, IEEE) received the B.S. degree in electronics engineering from Chosun University, in 2009, and the M.S. degree in electrical engineering from Chonnam National University, South Korea, in 2018, where he is currently pursuing the Ph.D. degree with the Department of Electrical Engineering. His research interests include the open fault detection and fault location for the distribution networks.

SEUNG-YOON HYUN received the M.S. degree in electronics engineering from Seoul National University, in 2018. From 2014 to 2020, he worked as a Professor at HQ and HRD Center in KEPCO. He is currently a Senior Researcher with the Smart Power Distribution Laboratory, KEPRI. He is responsible for establishing distribution operation strategies of KEPCO. His research interests include distribution protective coordination and strategy for future power systems.

YOUNG-WOO LEE (Member, IEEE) received the B.S. degree in electrical engineering from Chungbuk National University, Cheongju, South Korea, in 2010, and the Ph.D. degree in electrical engineering from Hanyang University, Seoul, South Korea, in 2017. In 2020, he joined the Faculty of Chonnam National University, Gwangju, South Korea. His main research interests include power system optimization, electric machine control, and nonlinear and optimal controller design.

JOON-HO CHOI (Member, IEEE) received the B.S., M.S., and Ph.D. degrees in electrical engineering from Soongsil University, Seoul, South Korea, in 1996, 1998, and 2002, respectively. Since 2003, he has been a Professor with Chonnam National University, Gwang-ju, South Korea. His research interests include operation and integration and control strategies of distributed generation and operation algorithms of the smart grid.

SEON-JU AHN (Member, IEEE) received the B.S., M.S., and Ph.D. degrees in electrical engineering from Seoul National University, Seoul, South Korea, in 2002, 2004, and 2009, respectively. He is currently a Professor at Chonnam National University, Gwangju, South Korea. His current research interests include power quality, distributed energy resources, microgrids, smart grids, and real-time simulation.

SANG-YUN YUN (Member, IEEE) received the B.S., M.S., and Ph.D. degrees in electrical engineering from Soongsil University, Seoul, South Korea, in 1996, 1998, and 2002, respectively. From 2002 to 2009, he was a Senior Researcher at the Electrotechnology Research and Development Center, LSIS, Cheongju, South Korea. From 2009 to 2016, he was a Principle Researcher at the KEPCO Research Institute, Daejeon, South Korea. He is currently a Professor at the Department of Electrical Engineering, Chonnam National University, Gwangju, South Korea. His research interests include the design of EMS, DMS and MGMS, and protection technologies for active distribution networks.